Computers and Fluids 160 (2018) 42–50

Contents lists available at ScienceDirect

Computers and Fluids

journal homepage: www.elsevier.com/locate/compfluid

Influence of travelling surface waves on nanofluidic viscosity

Jian-Fei Xie, Bing-Yang Cao*

Key Laboratory for Thermal Science and Power Engineering of Ministry of Education and Department of Engineering Mechanics, Tsinghua University, Beijing 100084, China

ARTICLE INFO

Article history:
Received 14 December 2016
Revised 18 October 2017
Accepted 22 October 2017
Available online 23 October 2017

Keywords:
Travelling surface wave
Nanofluidics
Viscosity
Molecular dynamics

ABSTRACT

The viscosity of nanofluidics in the presence of travelling surface wave has been investigated systematically by molecular dynamics (MD) simulations in this paper. The travelling surface wave propagating on the walls of nanochannel can affect the viscosity of nanofluidics sufficiently. The nanoscale fluid mechanism in nanochannels has been influenced by both amplitude and frequency of travelling surface wave, and the hydrodynamic characteristics have been affected significantly including the degree of boundary slip and mass flow rate (MFR). The MD results show that the viscosity of fluid at the nanoscale is an increasing function of the amplitude of travelling surface wave, but is reduced dramatically at the ultra-high frequency of travelling surface wave. The boundary slip illustrates the same trend as the variation of nanofluidic viscosity. For the mass flow rate, it depends on both the apparent viscosity of fluid and slip length at the boundary. Usually the viscosity and slip length are both independent on the pressure gradient, but are enlarged as the increment of pressure gradient in the presence of travelling surface wave. In contrast, when the travelling surface wave propagates on the walls of nanochannel, the mass flow rate is reduced as the pressure gradient increases. It has also been found that the viscosity, slip length and mass flow rate are influenced easily by the travelling surface wave on the hydrophobic surface (weak fluid-wall interaction). In addition, the stress distribution of fluid across the nanochannel has been shown, which indicates that the averaged total stress has been decreased under the condition of travelling surface wave. It can be concluded that our results provide the apparent viscosity of nanofluidics and hydrodynamic characteristics in the presence of travelling surface wave.

1. Introduction

Fast development and wide applications of nanotechnologies have been seen in the past two decades, and further understanding of the mass and momentum transport in nanoscale confinements that are dominated by the large surface area-to-volume ratio ($10^6 - 10^9$) is essential for a variety of applications: DNA profiling, optical filters and display technology, thermal management of semiconductor elements, and pollution monitoring [1–3]. Due to the large surface area-to-volume ratio, effects of the wall force field on liquids confined inside the nanoscale elements are significant, and the substantially different phenomena are observed, which are not expected in macroscale. Therefore, it is very necessary to investigate the nanoscale transport phenomena, and molecular dynamics (MD) simulations have emerged as a powerful tool for probing the microscopic behaviour of fluids, which can provide an accurate description of boundary condition at the molecular level and determination of fluid-wall interactions [4–8].

Particularly nanoscale confinements may induce significant changes in liquid viscosity. MD results have already indicated the viscosity dependence on the near-wall liquid distribution and wall structures [9–12]. Recently Ghorbanian and Beskok have reported the scale effects in nanochannel liquid flows [13], i.e., both channel averaged density and apparent viscosity decrease with the reduced channel height, which has competing effects in determination of the mass flow rate. Density layering and wall force field induce deviations from Newton's law of viscosity in the near-wall region. Their findings indicate that the size and wall force field significantly affect the hydrodynamics of nanoscale systems. On the other hand, experimental studies showed that on further decreasing the gap thickness by a single molecular layer, liquid films can undergo an abrupt transition and become a solid-like state in the sense that they are able to sustain a finite shear stress for macroscopic times. As a result, the effective rigidity of the films, which is represented by an effective creep viscosity, can be increased up to few orders of magnitude at the transition: viscosity may change with the confinement [14]. Another important aspect that changes the hydrodynamics of the nanoscale confinements is the velocity slip at the liquid-wall interface, which consequently influences the

* Corresponding author.
E-mail address: caoby@tsinghua.edu.cn (B.-Y. Cao).

https://doi.org/10.1016/j.compfluid.2017.10.022
0045-7930/

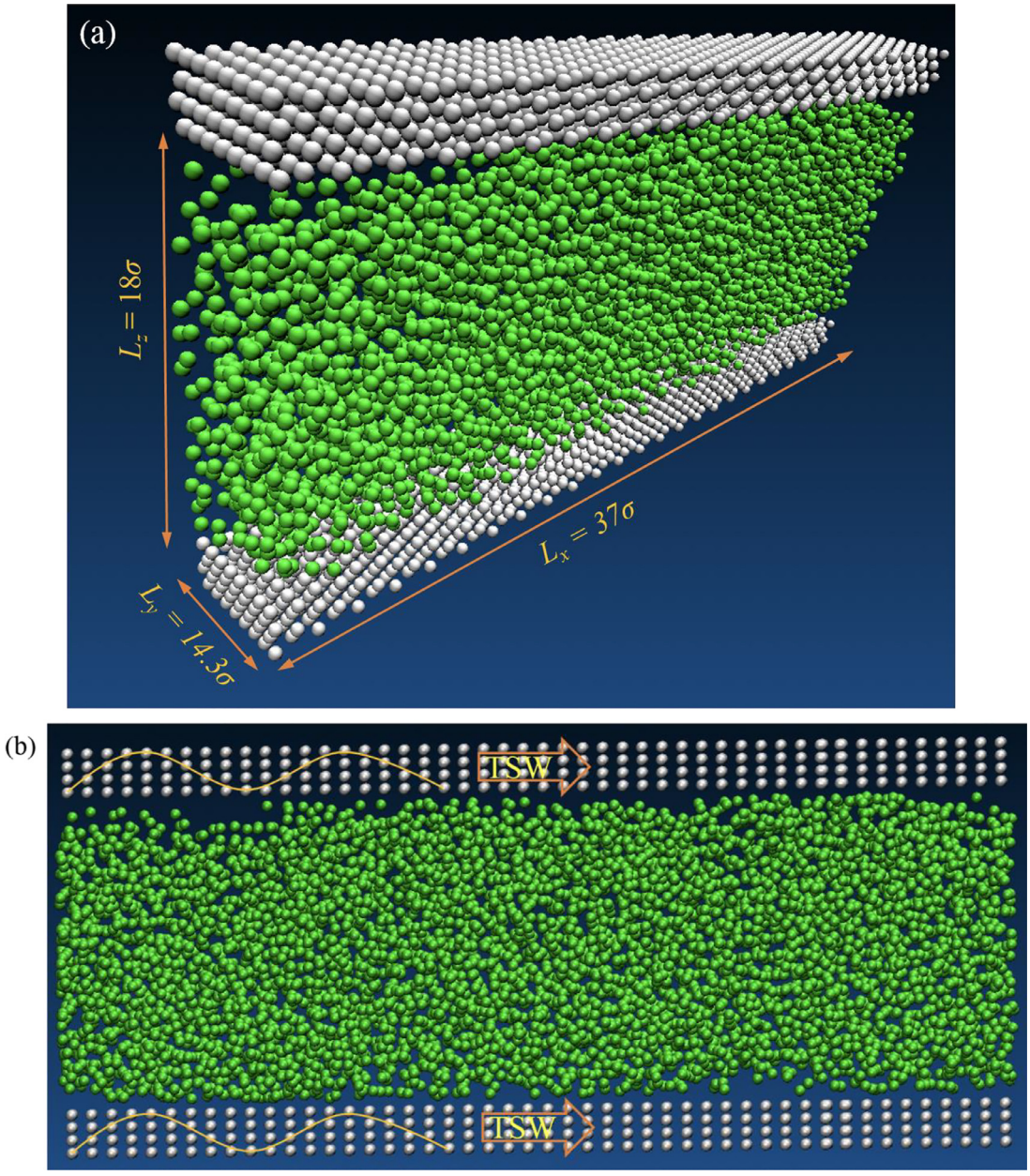

Fig. 1. Snapshot of nanochannel flow in the presence of travelling surface wave (a): channel length $L_x = 37\sigma$, $L_y = 14.3\sigma$ and channel height $H = 18\sigma$. Side view of nanochannel flow (b): the travelling surface waves (TSW) propagate on the walls of nanochannel along the positive direction of x axis. White atoms represent the wall atoms, and green ones are fluid molecules. The images were created using VMD [23]. (For interpretation of the references to colour in this figure legend, the reader is referred to the web version of this article.)

mass flow rate. Previous studies found that the degree of boundary slip is a function of the liquid viscosity and the shear rate [15], and the predicted slip length shows the linear dependence on viscosity [16].

In microfluidic biochip engineering, a driving force for driving microscale fluid motion has been introduced by employing the surface waves [17,18]. The key of this novel technology is to make a micropump that is able to position reagents on the surface of chips or in microfluidic channels without the mechanical contact. This is implemented in terms of the surface acoustic waves (SAW) that are induced using the radio frequency electric signals. In recent years, SAW technologies have attracted a lot of attention in microfluidics and nanofluidics community: biological/chemical sensing, micro/bioparticle manipulation schemes and on-chip droplet production [19–22]. Our recent findings also indicate that the fast nanofluidics can be induced by travelling surface waves. However, to the best of our knowledge, the fundamental of how travelling surface waves influence the viscosity of fluid in nanoscale confinements has not been explored, and the new hydrodynamics of nanoscale confinements resulting from the variations of fluid viscosity is less understood either.

In this paper, our purpose is to investigate the effect of travelling surface waves on the apparent viscosity of nanofluidics by MD simulations. The theoretical prediction of the force driven flow is presented in the next section. MD techniques and the application of travelling surface waves are introduced in Section 3. The nanoscale hydrodynamics of fluid flowing through nanochannels in the presence of travelling surface waves are investigated in Section 4, and the influence of travelling surface waves on the ap-

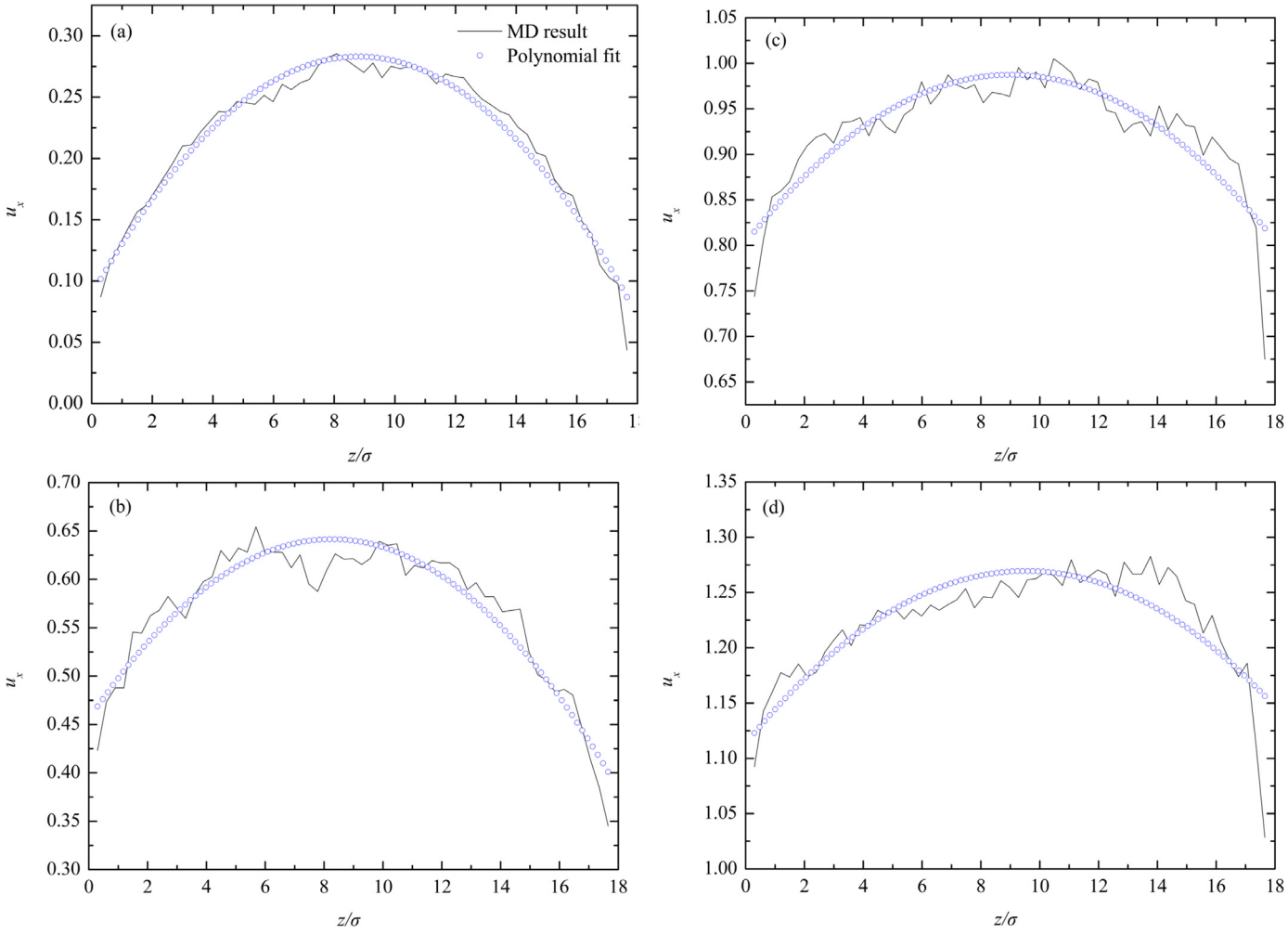

Fig. 2. Velocity profiles in the nanochannel in the presence of travelling surface wave: (a) $u_0 = 0$, i.e., without applying the travelling surface wave; (b) $u_0 = 0.01$; (c) $u_0 = 0.02$; and (d) $u_0 = 0.03$. The second-order polynomial relation is used to fit the MD data.

parent viscosity of fluid is also shown. The conclusions are drawn in Section 5.

2. Theoretical formation

A force driven flow has been carried out to investigate the viscosity of fluid in the nanochannel, and the fluid is confined between two solid planar walls parallel to the *xy* plane with periodic boundary conditions imposed along the *x* and *y* directions, which is shown in Fig. 1(a). The simulated characteristic length, i.e., the distance between the two plates, reaches $H = 18\sigma$ (σ is the diameter of fluid molecule), which is really comparable with the characteristic size of NEMS devices in engineering situations. The size of the simulation cell in the x and y directions is $L_x = 37\sigma$ and $L_y = 14.3\sigma$, respectively. Poiseuille flow is driven by a pressure gradient along the *x* direction, and is locally fully developed (LFD) to be laminar with small Reynolds numbers. In the case of the planar Poiseuille flow of a Newtonian fluid under the constant external force, the macroscopic hydrodynamics gives a parabolic solution of the Navier–Stokes (NS) equation. Considering the slip boundary condition, the velocity profile of a LFD flow may be written as [24]

$$u(z) = -\frac{\rho g}{2\mu}z^2 + \frac{\rho g H}{2\mu}z + u_s, \tag{1}$$

where ρ is the density of fluid, μ is the dynamical viscosity, u_s is the slip velocity of fluid on the solid surface, and g is the acceleration factor. The force driven flow is implemented by applying the acceleration factor to each fluid molecule in our investigation. The velocity slip can be easily obtained through analysing the velocity profile. According to the Navier boundary condition [25], the slip length l_s can be calculated by extrapolating the velocity profiles from the position in the fluid to where the velocity would vanish

$$u_s = l_s \frac{du}{dz}\Big|_{z=0}. \tag{2}$$

It should be noted that the wall is located at $z = 0$. On the basis of boundary condition given by Eq. (2), the governing Eq. (1) can be rewritten as follows

$$u(z) = -\frac{\rho g}{2\mu}z^2 + \frac{\rho g H}{2\mu}z + \frac{\rho g H l_s}{2\mu}. \tag{3}$$

If the governing equation is expressed in the form of a second-order polynomial relation $u(z) = a_2 z^2 + a_1 z + a_0$, one has $a_1 = -\frac{\rho g}{2\mu}$, $a_2 = \frac{\rho g H}{2\mu}$ and $a_0 = -\frac{\rho g H l_s}{2\mu}$. Therefore, the viscosity of fluid can be calculated by $\mu_1 = -\frac{\rho g}{2a_2}$. Furthermore, following the approach that Ghorbanian and Beskok have proposed [13], the viscosity of fluid can be estimated as follows. We use the maximum velocity u_{max} that occurs at the centre of the nanochannel and find a coefficient a_2 from $u(z) = a_2 z\ (z - H)$ as $a_2 = -|\frac{4u_{max}}{H^2}|$, and

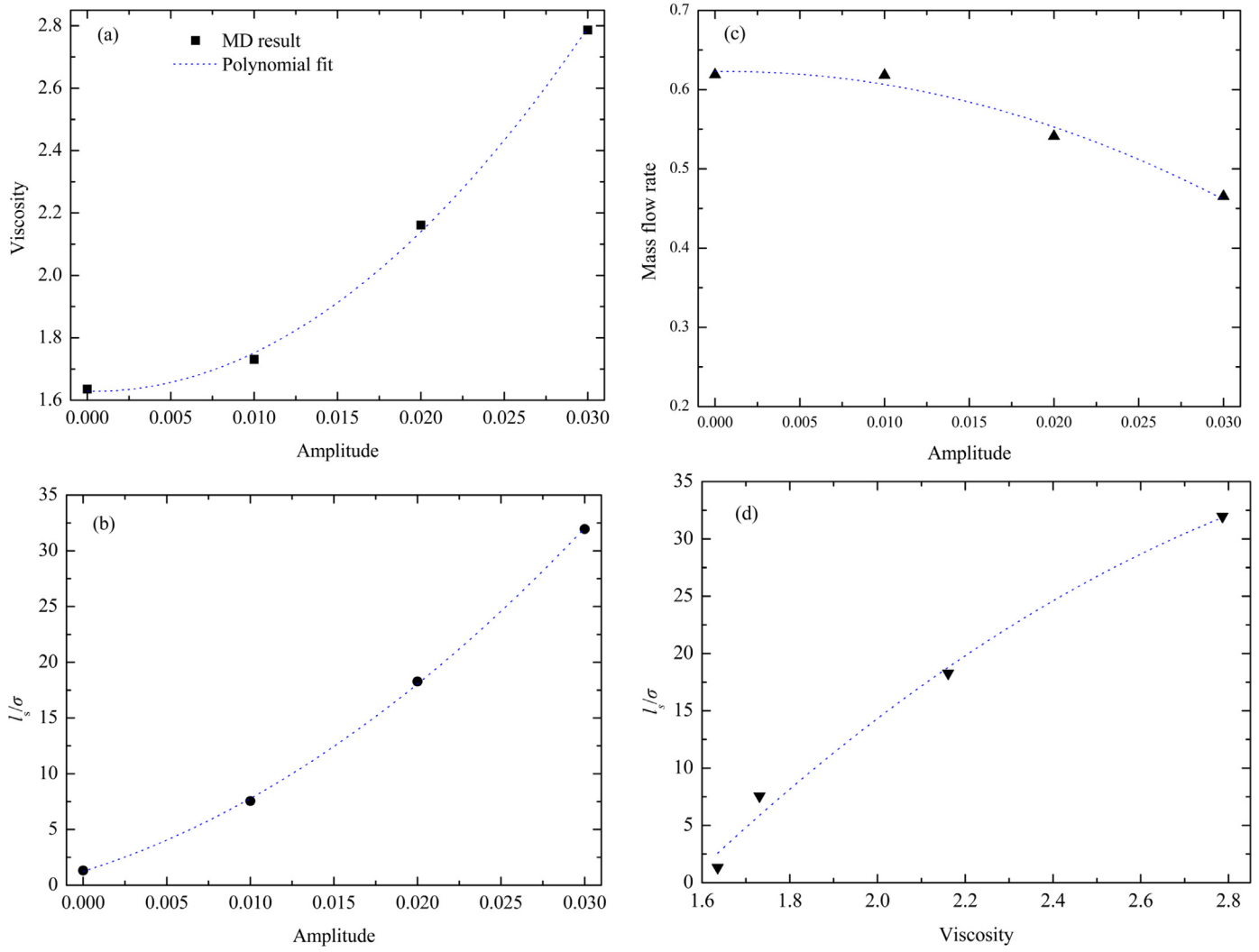

Fig. 3. Fluid viscosity, slip length and mass flow rate as a function of amplitude of travelling surface wave (a)–(c). In addition, the slip length as a function of the fluid viscosity is plotted (d). The second-order polynomial relation is used to fit the MD data.

then calculate viscosity using the same formula $\mu_2 = -\rho g/2a_2$ as other researchers usually do. As a result, we define the apparent viscosity [26] of fluid as the average of the two values. It can be concluded that the apparent viscosity is predicted using a parabolic fit to the streaming velocity profile. On the other hand, the diffusion coefficient for liquid molecules is derived from the Einstein diffusion formula [27], and the viscosity can be calculated alternatively by the Green–Kubo form [11,28,29]. As the velocity distribution of fluid flowing through the nanochannel is known, the mass flow rate (MFR) can be obtained by integrating the velocity profile across the nanochannel with respect to the constant density of fluid ρ and uniform channel width L_y as follows

$$\dot{m} = \rho L_y \int_0^H u(z)dz = \frac{\rho^2 g L_y H^3}{12\mu}\left(1 + 6\frac{l_s}{H}\right). \tag{4}$$

It can be known that the mass flow rate is proportional to the slip length, but inversely proportional to the viscosity of fluid. The variation of mass flow rate as a function of flow characteristics in the presence of travelling surface wave will be discussed later. Both Eqs. (1) and (4) assume a constant density of fluid, but it should be noted that the non-uniform distribution of fluid density may be expected in the channel and the condensed layer of fluid near the wall could be destroyed in the presence of travelling surface waves [30].

3. Molecular simulations and travelling surface waves

The liquid argon is confined in the nanochannel, and argon molecules interact through a Lennard–Jones (LJ) potential

$$V(r_{ij})^{LJ} = \begin{cases} 4\varepsilon\left[\left(\frac{\sigma}{r_{ij}}\right)^{12} - \left(\frac{\sigma}{r_{ij}}\right)^{6}\right], & r_{ij} \ll r_c \\ 0, & r_{ij} > r_c \end{cases}, \tag{5}$$

where r_{ij} is the intermolecular distance, and r_c is the cutoff distance, respectively. The length and energy scales are chosen as $\sigma_A = 3.405 \times 10^{-10}$ m and $\varepsilon_A = 1.67 \times 10^{-21}$ J. Other simulation parameters such as the molecular mass m_A and natural time unit τ can be found in [31]. A leapfrog Verlet algorithm with a time step of $\Delta t = 0.002\tau$ is applied to solve the equations of motion. In addition, we take $r_c = 2.5\sigma$ and use the cell-linked list method to reduce the computational time [32]. The equilibrium state of the fluid is well defined liquid phase characterized by number density $\rho = 0.8\sigma^{-3}$ and temperature $T = 1.1k_B/\varepsilon_A$, where k_B is the Boltzmann constant. The velocity rescaling technique is applied to wall atoms to maintain a constant wall temperature, and the fluid

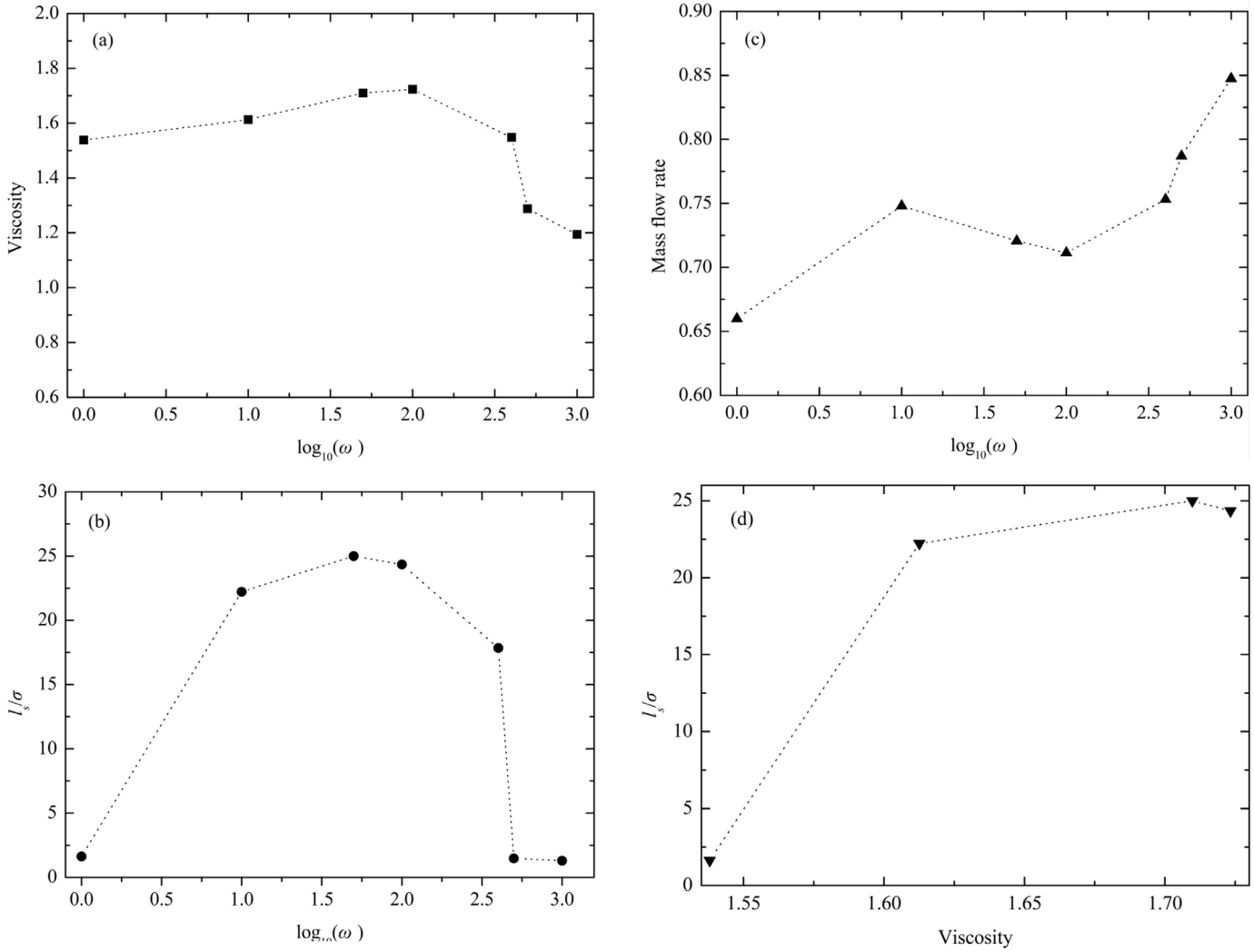

Fig. 4. Fluid viscosity, slip length and mass flow rate as a function of frequency of travelling surface wave (a)–(c). In addition, the slip length as a function of the fluid viscosity is plotted (d).

system is kept at a constant temperature by a Langevin thermostat method in the z direction [33]. The velocity shear rate at the boundary of nanochannel flow is kept much smaller than the critical value $\dot{\gamma} \sim (m\sigma_{AP}^2/\varepsilon_{AP})^{-1/2}$, which can guarantee that the slip length at the boundary is independent of the driving field in our MD simulations [34]. The region between the two planar walls is divided into bins along the z direction to obtain running averages for the fluid properties such as density and velocity.

Now we focus on the solid walls of nanochannel, each of which consists of atoms forming two planes of a face-centred cubic (FCC) lattice. To maintain a well-defined solid structure with a minimum number of solid atoms, each wall atom is attached to a lattice site with a spring. Based on the Einstein theory, each wall atom vibrates around the FCC lattice site with the Einstein frequency by a harmonic spring with stiffness $\kappa = 16\pi^4 k_B^2 m\theta^2/\hbar^2$, where $\hbar$ is the Plank constant, m is the mass of a wall atom, and $\theta = 180\,\mathrm{K}$ is the Einstein temperature [35]. The spring constant is used to control the thermal roughness of the wall and its responsiveness to the fluid. The fluid-wall (argon-platinum) interaction is also modelled with the LJ potential, and is expressed as follows

$$V(r_{ij})_{AP} = 4c\varepsilon_{AP}\left[\left(\frac{\sigma}{r_{ij}}\right)^{12} - \left(\frac{\sigma}{r_{ij}}\right)^{6}\right], \tag{6}$$

in which the constant c is used to control the interaction strength between the fluid molecules and wall atoms, i.e., surface wettability, and larger values of c refer to as the stronger interactions between fluid molecules and wall atoms (hydrophilic surface). The length and energy scales $\sigma_{AP} = 3.085 \times 10^{-10}\,\mathrm{m}$ and $\varepsilon_{AP} = 0.894 \times 10^{-21}\,\mathrm{J}$ are obtained in terms of Lorentz-Berthelot rule [27,32]. It should be noted that the MD algorithm presented here has been applied to both gas and liquid flows in our previous works [25,30,31].

In particular, the travelling surface wave is generated and propagates on the walls of nanochannel along the x direction. The perturbation to the wall atoms is governed by [36]

$$u = u_0 \cos(\omega t - kx), \tag{7}$$

where u_0, $\omega = 2\pi/T$ and T are the amplitude, frequency and period of the travelling surface wave, respectively. Parameter k corresponds to the spatial frequency of the travelling surface wave, and is related to the wavelength λ by $k = 2\pi/\lambda$. Since the current MD investigations are focused on the Rayleigh surface-travelling wave and its effect on the physical phenomenon of nanoscale flows, the longitudinal component of the displacement is given only. Moreover, the exponential decay of transverse displacement is negligible due to the limited size of nanochannel, resulting that the perturbation of wall atoms follows the form of travelling surface

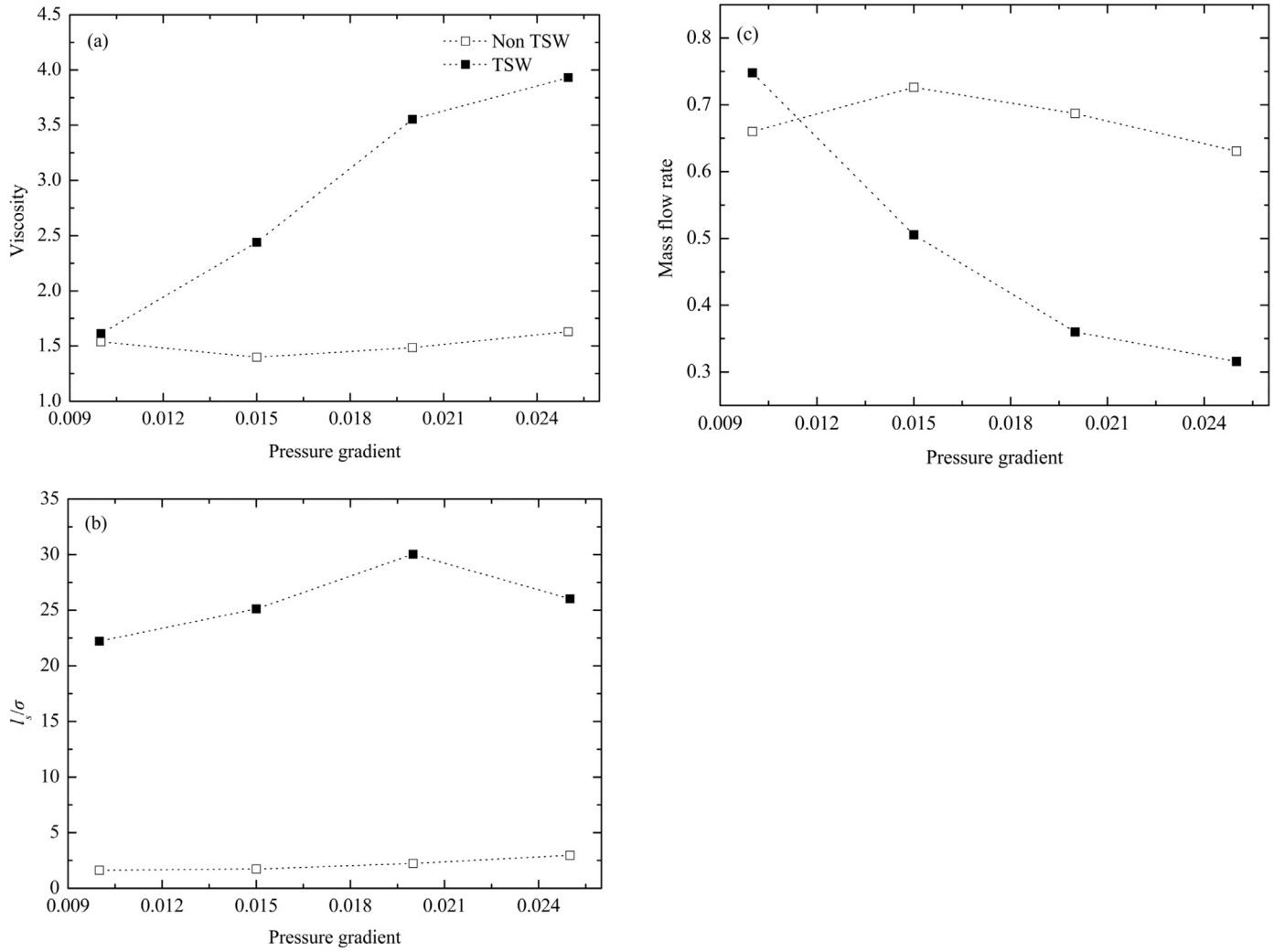

Fig. 5. Fluid viscosity, slip length and mass flow rate as a function of pressure gradients (a)–(c) in the presence of travelling surface wave. Open squares represent the case without applying the travelling surface wave, and filled ones represent the case in the presence of travelling surface wave.

Table 1
Physical parameters in MD simulations.

Parameter	Symbol	Value
Diameter	σ_A	3.405×10^{-10} m
	σ_{AP}	3.085×10^{-10} m
Energy	ε_A	1.67×10^{-21} J
	ε_{AP}	0.894×10^{-21} J
Mass	m_A	40 a.u.
	m_P	195 a.u.
Time	τ	2.15×10^{-12} s
Temperature	ε_A / k_B	119.8 K
Density	ρ	$0.8\, m_A/{\sigma_A}^3$

Table 2
Influence of bin width on the viscosity of fluid.

Bin width	μ_1	μ_2	μ_{av}
0.6	1.6	1.3736	1.4868
0.4	1.4815	1.5423	1.5119
0.3	1.4815	1.5123	1.4969
0.24	1.4815	1.5225	1.502
0.2	1.4815	1.5239	1.5027

wave. Importantly imposing the travelling surface wave physically requires a proper phase velocity, i.e., $\omega\lambda/2\pi$, to guarantee $N\lambda$ on the walls, where N is a positive integer. For example, a phase velocity of 3444 m s^{-1} is chosen to get 6λ along with the longitudinal length of nanochannel $L_x = 12.6$ nm. It is noted that all dimensional quantities such as the fluid density ρ and velocity u given by the LJ unit in MD simulations will be understood to be multiplied by an appropriate combination of σ_A, ε_A and m_A, which are shown in Table 1.

4. Results and discussion

Before we are to determine the viscosity of fluid in the nanochannel, the effect of bin width on the calculation of this characteristic has been investigated. To do so, five values of bin width have been adopted to compute the viscosity of fluid confined in the nanochannel, and the bin-width dependence of fluid viscosity is shown in Table 2. As can be seen in Table 2, the fluid viscosity is independent on the bin width when it is equal to 0.3σ or smaller, and therefore the value of 0.3σ has been chosen in our MD simulations. In addition, the density layering near the walls of nanochannel cannot be captured exactly if the bin width is greater than 0.4σ (Results not shown for brevity), which will result in the inaccurate estimate of kinetic contributions to stress tensor [13]. Koplik *et al* suggested that the num-

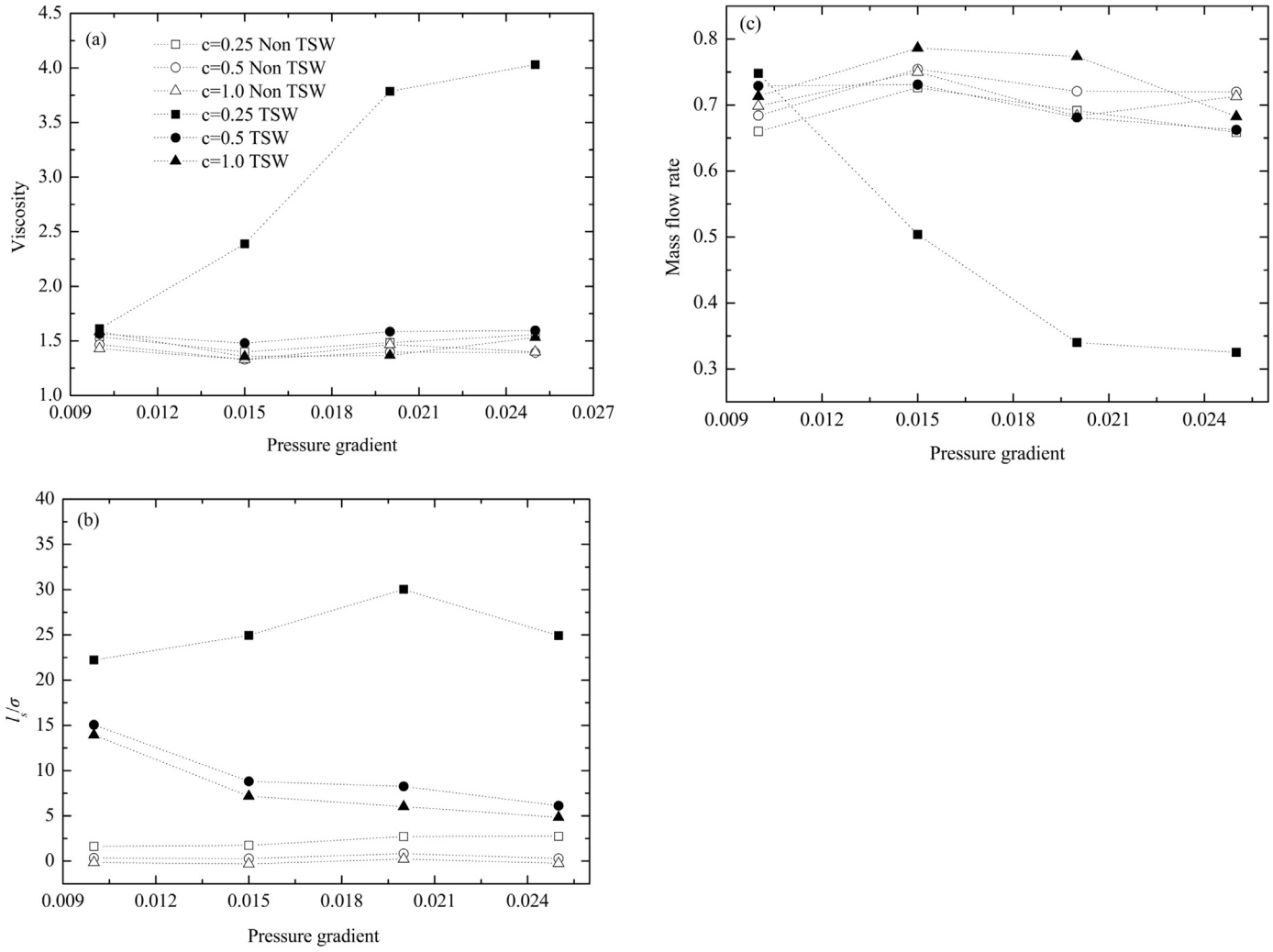

Fig. 6. Fluid viscosity, slip length and mass flow rate as a function of fluid-wall interactions (a)–(c) in the presence of travelling surface wave. Open symbols represent the case without applying the travelling surface wave, and filled ones represent the case in the presence of travelling surface wave.

ber of bin is usually equal to twice the number of unit cells of the initial FCC lattice giving a bin width $O(\sigma)$ [37], which is one order larger in magnitude than our predicted value. As can be seen in Fig. 1(b), the condensed layer of fluid molecules disappears when the travelling surface waves propagate on the walls of nanochannel, and the motion of fluid molecules near the walls forms the frame of travelling surface wave in some ways.

The effect of amplitude of the travelling surface wave on the velocity profiles of fluid flowing through the nanochannel is shown in Fig. 2 including three values of amplitude, i.e., $u_0 = 0.01$, 0.02 and 0.03 ($\omega = 10$, $c = 0.25$, and $g = 0.01$). As shown in Fig. 2, the average velocity across the nanochannel is increased as the amplitude increases. In addition, on the basis of Eqs. (2) and (3), Fig. 3 shows the variations of hydrodynamic characteristics as a function of amplitude. Fig. 3(a) indicates that the viscosity of fluid is an increasing function of the amplitude. As can be seen in Fig. 3(b), the slip length of fluid on the walls of nanochannel is also increased with the increase of amplitude, and is enlarged more than 10 times at the large amplitude than that without applying the travelling surface wave. The mass flow rate, however, is decreased as the amplitude increases, which is shown in Fig. 3(c). According to Eq. (4), we know that the mass flow rate is proportional to the slip length, but is inversely proportional to the viscosity of fluid. Fig. 3(c) illustrates that the increase of fluid viscosity contributes more to the reduction of mass flow rate. Moreover, the variation of slip length as a function of the fluid viscosity is shown in Fig. 3(d), indicating that the slip length is an increasing function of fluid viscosity. It had also been reported that the degree of boundary slip is a function of the liquid viscosity [15], and the slip length shows the predicted linear dependence on viscosity [16].

The second aspect is the effect of frequency of travelling surface wave on the viscosity of fluid, and the range of frequency from 10 to 1000 has been taken into account ($u_0 = 0.01$, $c = 0.25$, and $g = 0.01$). Fig. 4(a) shows the variation of fluid viscosity as a function of frequency of travelling surface wave. The viscosity of fluid is not a monotonic function of frequency of travelling surface wave as found for amplitude in Fig. 3(a). Instead, the viscosity of fluid increases slightly as the frequency increases and reaches the maximum value at $\omega = 100$. Then the viscosity of fluid decreases dramatically while the frequency continues increasing. The slip length shows the same trend as the variation of fluid viscosity, that is, the boundary slip increases with the increase of frequency until it reaches its peak at $\omega = 50$, and drops significantly with the increase of frequency, which is shown in Fig. 4(b). In addition, the viscosity of fluid is equal to its value without applying the travelling surface wave when the frequency exceeds 500. The influence of frequency on the mass flow rate is more complicated. As can be seen in Fig. 4(c), the mass flow rate increases under the low frequency and keeps almost unchanged under the medium frequency. However, the mass flow rate is increased dramatically un-

der the ultra-high frequency. The slip length on the surface shows a monotonic increasing function of fluid viscosity, which is shown in Fig. 4(d), and the degree of boundary slip is comparable to that under the amplitude of travelling surface wave.

It is known that the external force driven flow is dependent on the pressure gradient significantly, and its effect on the viscosity of fluid in the presence of travelling surface wave seems important. As can be seen in Fig. 5(a), without imposing the travelling surface wave on the walls of the nanochannel the viscosity of fluid is independent on the pressure gradient, which indicates that the fluid remains Newtonian. The viscosity of fluid, however, has been enlarged significantly in the presence of travelling surface wave. The same variation is found for the slip length of fluid flow on the walls, which is shown in Fig. 5(b), i.e., the slip length is increased significantly in the presence of travelling surface wave when the pressure gradient increases, but is independent on the pressure gradient without applying the travelling surface wave. The variation of mass flow rate as a function of pressure gradient seems more complicated whether the travelling surface waves propagate on the walls of nanochannel or not. Fig. 5(c) shows that the mass flow rate increases slightly with the increase of pressure gradient in the absence of travelling surface wave, but falls when the pressure gradient continues increasing. On the other hand, the mass flow rate has been reduced dramatically in the presence of travelling surface wave as the pressure gradient increases. It can be concluded again that the mass flow rate in the nanochannel depends on both the viscosity of fluid and slip length on the wall.

For small scale phenomena such as the nanochannel flows, the wall force field, i.e., the fluid-wall interaction (FWI), plays an important role in the hydrodynamic characteristics [13,31]. In this paper, three magnitudes of fluid-wall interactions are considered, i.e., $c = 0.25$, 0.5 and 1.0 are taken into account ($u_0 = 0.01$ and $\omega = 10$), which refer to as the weak, medium and strong wetting surfaces, respectively. As can be seen in Fig. 6(a), without imposing the travelling surface wave on the walls of nanochannel the viscosity of fluid keeps constant on whatever the solid surface, hydrophobic (weak FWI) or hydrophilic (strong FWI), which indicates the Newtonian behaviour. Moreover, the viscosity of fluid also shows unchanged under the medium and strong FWI, but is increased dramatically on the hydrophobic surface in the presence of travelling surface wave. The slip length of fluid on the wall keeps the level under the three FWI in the absence of travelling surface wave, which is shown in Fig. 6(b) and consistent with the observation in Fig. 5(b). On the other hand, the variation of slip length shows more complicated when the travelling surface wave is imposed on the walls of nanochannel. As shown in Fig. 6(b), the slip length is decreased on the hydrophilic surfaces (medium and strong FWI) as the pressure gradient increases. However, when the solid surface becomes hydrophobic, i.e., the weak FWI, the slip length increases slightly with the increase of pressure gradient. Combining with observations in Fig. 6(a) and (b), we may conclude that the hydrodynamic characteristics of fluid flowing through the nanochannel in the presence of travelling surface wave could be affected more significantly on the hydrophobic surface. Furthermore, Fig. 6(c) illustrates that under the condition of the travelling surface wave propagating on the walls of nanochannel the mass flow rate is reduced dramatically on the hydrophobic surface (weak FWI) with the increase of pressure gradient, but is affected insignificantly under the medium or strong FWI whether the travelling surface wave is imposed on the walls of nanochannel or not.

Investigations of the viscosity of fluid in the nanochannel indicate the non-Newtonian behaviour in the presence of travelling surface wave. In particular the viscosity of fluid is increased significantly on the hydrophobic surface, i.e., the weak fluid-wall interaction. Therefore, the constitutive relation is more concerned, and the stress tensor of fluids flowing through the nanochannel has

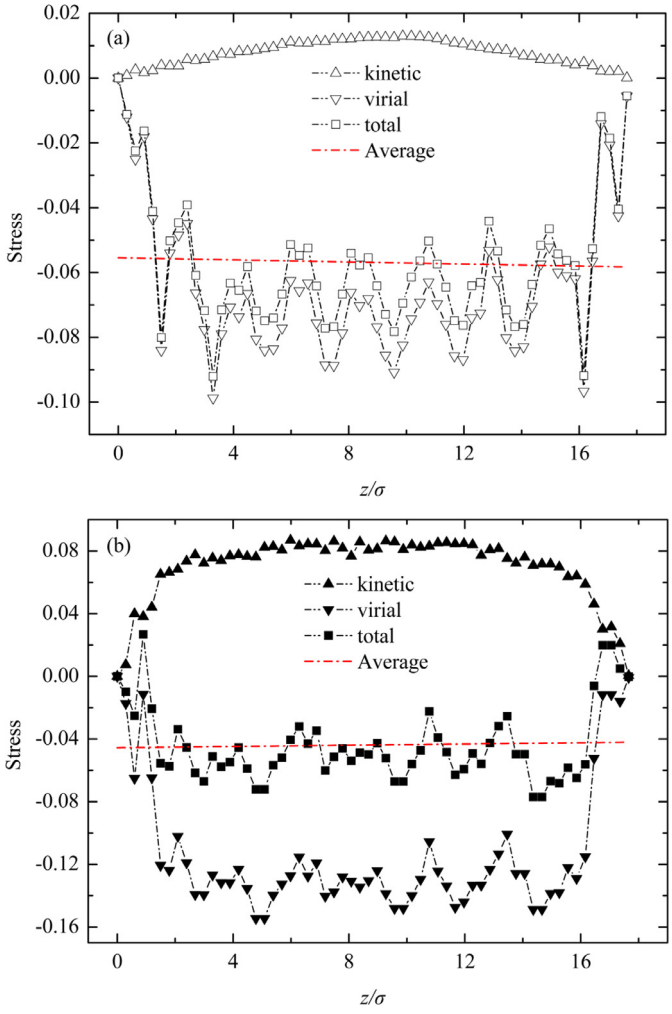

Fig. 7. Stress distribution of fluid flow across the nanochannel: (a) without applying the travelling surface wave and (b) in the presence of travelling surface wave. The red-dotted line represents the total stress averaged within the bins. (For interpretation of the references to colour in this figure legend, the reader is referred to the web version of this article.)

been computed from the molecular trajectories using the Irving–Kirkwood expression as follows [38]

$$T = \sum_i m_i \left(\frac{d\mathbf{x}_i}{dt} - \mathbf{u} \right) \left(\frac{d\mathbf{x}_i}{dt} - \mathbf{u} \right) + \frac{1}{2} \sum_{i,j} r_{ij} \mathbf{F}_{ij}, \tag{8}$$

in which $\mathbf{u}$ is the local average velocity and $\mathbf{F}$ is the force between the two molecules. The first term on the right-hand side of Eq. (8) is the kinetic component, and the second term is the virial component, respectively. The kinetic term in the Irving–Kirkwood expression is related to the ideal-gas law, whereas the particle-particle virial terms are corrections to the ideal gas law because of the interaction of particles having non-zero volumes and force fields [6]. Accurate prediction of pressure, and hence, the thermodynamic state for liquids require taking into account the long-range force field interactions between the particles, i.e., long range corrections [32]. Fig. 7(a) shows the stress distribution of fluid flow across the nanochannel including the kinetic and virial contributions in the absence of travelling surface wave. As can be seen in Fig. 7(a), the virial component plays an important role in the stress distribution, and is quite close to the total stress. In contrast, the kinetic component of stress is increased significantly when the travelling surface waves propagate on the walls of nanochannel, which is shown in Fig. 7(b), and the resulting total stress is

smaller than that in the absence of travelling surface wave. The averaged values of total stress are −0.55 and −0.5 for the two cases, respectively. It can be explained that the momentum exchange has been implemented sufficiently between the fluid and travelling surface wave resulting in the increase of kinetic component of the stress when the travelling surface wave is imposed on the walls of nanochannel.

5. Conclusion

In this paper, we have investigated the viscosity of nanofluidics in the presence of travelling surface wave systematically using molecular dynamics (MD) simulations. Our MD results showed that the travelling surface wave propagating on the walls of nanochannel can affect the viscosity of nanofluidics sufficiently, and the nanoscale fluid mechanism in nanochannels was influenced by both amplitude and frequency of travelling surface wave. The viscosity of fluid at the nanoscale was an increasing function of the amplitude of travelling surface wave, but was reduced dramatically at the ultra-high frequency of travelling surface wave.

The hydrodynamic characteristics such as the slip length and mass flow rate (MFR) had also been affected significantly by the travelling surface wave. The slip length at the fluid- wall interface showed the same trend as the variation of nanoscale viscosity in the presence of travelling surface wave. For the mass flow rate, it was proportional to the slip length, but was inversely proportional to the viscosity of fluid. It was found that the effect of pressure gradient on the viscosity and slip length of the external force driven flow can be ignored in the absence of travelling surface wave. However, they were increased as the pressure gradient increased under the condition of travelling surface wave propagating on the walls of nanochannel. In contrast, the mass flow rate was a decreasing function of the pressure gradient due to the greater contribution of nanofluidic viscosity. In nanoflows the wall force field (fluid-wall interaction) also played an important role, and its effect on the viscosity, slip length and mass flow rate was found to be significant on the hydrophobic surface (weak fluid-wall interaction) in the presence of travelling surface wave. Furthermore, the distribution of stress tensor of fluid across the nanochannel indicated that the averaged total stress was decreased by the momentum exchange between the fluid and travelling surface wave. It can be concluded that our results provide the apparent viscosity of nanofluidics and hydrodynamic characteristics in the presence of travelling surface wave.

Acknowledgments

The support of the National Natural Science Foundation of China (Grants No. 51506110 and 51676108) and Science Fund for Creative Research Groups (No. 51621062) was gratefully acknowledged.

References

[1] Insepov Z, Wolf D, Hassanein A. Nano Lett 2006;6:1893.
[2] Cecchini M, Girardo S, Pisignano D, Cingolani R, Beltram F. Appl Phys Lett 2008;92:104103.
[3] Roosta S, Nikkhah SJ, Sabzali M, Hashemianzadeh SM. RSC Adv 2016;6:9344.
[4] Koplik J, Banavar JR. Annu Rev Fluid Mech 1995;27:257.
[5] Kikugawa G, Takagi S, Matsumoto Y. Comput Fluids 2007;36:69.
[6] Barisik M, Beskok A. Microfluid Nanofluid 2011;11:269.
[7] Liang T, Ye W. Commun Comput Phys 2014;15:246.
[8] Reinhold J, Veltzke T, Wells B, Schneider J, Meierhofer F, Ciacchi LC, et al. Comput Fluids 2014;97:31.
[9] Sokhan VP, Nicholson D, Quirke N. J Chem Phys 2002;117:8531.
[10] Thomas JA, McGaughey AJH. Nano Lett 2008;8:2788.
[11] Suk ME, Aluru NR. RSC Adv 2013;3:9365.
[12] Lou Z, Yang M. Comput Fluids 2015;117:17.
[13] Ghorbanian J, Beskok A. Microfluid Nanofluid 2016;20:1.
[14] Klein J, Kumacheva E. J Chem Physics 1998;108:6996.
[15] Craig VSJ, Neto C, Williams DRM. Phys Rev Lett 2001;87:054504.
[16] Lichter S, Martini A, Snurr RQ, Wang Q. Phys Rev Lett 2007;98:226001.
[17] Koster D. Siam J Sci Comput 2007;29:2352.
[18] Mao ZM, Xie YL, Guo F, Ren LQ, Huang PH, Chen YC, et al. Lab Chip 2016;16:515.
[19] Guo YJ, Lv HB, Li YF, He XL, Zhou J, Luo JK, et al. J Appl Phys 2014;116.
[20] Zhou J, DeMiguel-Ramos M, Garcia-Gancedo L, Iborra E, Olivares J, Jin H, et al. Sens Actuat B Chem 2014;202:984.
[21] Nama N, Barnkob R, Mao ZM, Kahler CJ, Costanzo F, Huang TJ. Lab Chip 2015;15:2700.
[22] Brenker JC, Collins DJ, Van Phan H, Alan T, Neild A. Lab Chip 2016;16:1675.
[23] Humphrey W, Dalke A, Schulten K. J Mole Graph 1996;14:33.
[24] Morris DL, Hannon L, Garcia AL. Phys Rev A 1992;46:5279.
[25] Xie J-F, Cao B-Y. AIP Adv 2016;6:075307.
[26] Pritchard PJ. Fox and Mcdonald's introduction to fluid mechanics. NJ: John Wiley & Sons, Inc.; 2011.
[27] Rapaport DC. The art of molecular dynamics simulation. Cambridge: Cambridge University Press; 1995.
[28] Meier K, Laesecke A, Kabelac S. J Chem Phys 2004;121:3671.
[29] Thomas JA, McGaughey AJH. Nano Lett 2008;8:2788.
[30] Xie J-F, Cao B-Y. Microfluid Nanofluid 2017;21:111.
[31] Xie J-F, Cao B-Y. Mole Simul 2017;43:65.
[32] Allen MP, Tildesley DJ. Computer simulation of liquids. Oxford: Clarendon; 1987.
[33] Thompson PA, Robbins MO. Phys Rev Lett 1989;63:766.
[34] Thompson PA, Troian SM. Nature 1997;389:360.
[35] Cao BY, Chen M, Guo ZY. Appl Phys Lett 2005;86:091905.
[36] Worden K. Strain 2001;37:167.
[37] Koplik J, Banavar JR, Willemsen JF. Phys Fluids A 1989;1:781.
[38] Irving J, Kirkwood J. J Chem Phys 1950;18:817829.